Kaspars KROICS[1], Ugis SIRMELIS[1] Viesturs BRAZIS[2]

Institute of Physical Energetics (1), Riga Technical University (2)

Design of coupled inductor for interleaved boost converter

Abstract. *This paper presents an analysis of coupled inductor for interleaved boost converter and the effect of coupled inductor on current ripple reduction and on load transient response time. From the analysis a ETD core based coupled inductor structure is proposed to maximize the performance of the DC-DC converter. The inductor can be designed in convenient way by using commercially manufactured coil formers and ferrite cores.*

Streszczenie. *W artykule zaprezentowano analizę sprzężonego dławika stosowanego w przekształtniku typu boost w celu tłumienia tętnień i poprawy stanów przejściowych. Zaproponowano strukturę typu ETD.* ***Projekt sprzężonego dławika w zastosowaniu do przekształtnika typu boost****.*

Keywords: coupled inductor, boost converters, interleaved converters.
Słowa kluczowe: przekształtnik typu boost, dławik.

doi:10.12915/pe.2014.12.21

Introduction

In many applications such as photovoltaic arrays, fuel cells, wind generators high efficiency, small size boost DC-DC converter are required as an interface between the low voltage source and the output loads, which operates at higher voltages. Particular converter is proposed to match output voltage of wind generator with input voltage of the industrial AC inverter.

Figure 1 [1] shows the normalized output current ripple according to number of phases (N_{PH}) and duty cycle. It shows that by using interleaved structure current ripple can be significantly reduced. In given case duty cycle is changing from 40% to 60% therefore 4 phase boost converter structure is selected.

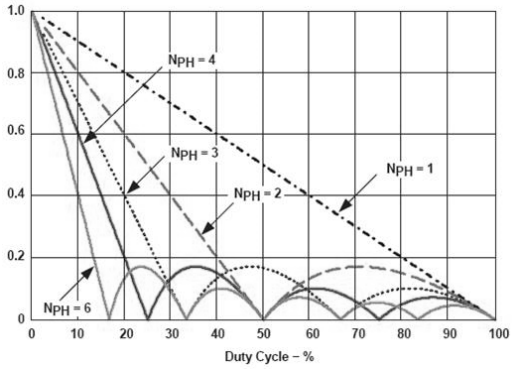

Fig. 1. Normalized output current ripple of boost converter

Figure 3 shows the structure of the boost DC-DC converter. The transistors VT1 to VT4 is controlled by pulse width modulation. The switching frequency of the converter is selected to 50 kHz. The four phase boost converter consists of four single boost converters that are connected in parallel as shown in Fig 2. Each parallel switch turns ON with shifting of 90 degrees. One of the major advantages of the multiphase converter is the ripple cancellation effect, which enables the use of a small inductance to improve the transient response and to minimize the input and output capacitances.

To control DC/DC converter digital control is used. Digital controllers of the previous era had bandwidth problems. In the recent years the situation has changed significantly. The speed and functionality performance of the microcontrollers has improved. They are also available at a much lower cost. The advantage of the digital controller is that it is programmable and offers more functionality to the system compared to the analog controllers. Novel control algorithms and methods with digital control can be realized.

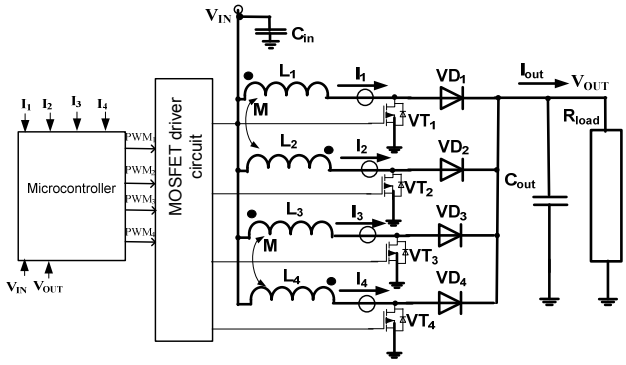

Fig. 2. The schematics of the interleaved DC-DC converter

Interleaving control schemes are widely used in converter applications [2, 3, 4]. Merits of such control methods are reduction of input/output current or voltage ripples and volume, and increase in the processed power capacity of converters.

In order to reduce inductor current ripple as well as output current ripple the two inductors should be coupled in some way. The research on the interleaved DC-DC converters using coupled inductor is reflected in [5]-[9]. Coupled inductor is a special form of multiple winding coupled magnetic structure. The advantages of integrated magnetic techniques are that amount of core material is reduced. The significant advantage of interleaved converter with coupled inductor is that the ripple in one winding can be dumped to another winding.

Design of coupled inductor

The interleaving structure has more inductors than the single phase converter. The two individual inductors of the two interleaving channels can be integrated on a single magnetic core to reduce component size. The structure of the integrated inductor is shown in Fig. 3. The both windings of the inductors is built on the central leg of the E core. Although in literature [5] is proposed to place windings of the inductor on the wing legs thereby obtaining higher leakage inductance, it is not available commercially manufactured coil formers for such a case. In this paper proposed inductor can be wound on ETD39 coil former in a convenient way. Figure 4 shows practical implementation of the coupled inductor of two phases. Winding of the one phase (2) and winding of the phase (3) electrically shifted in phase by 180 degree are separated by isolating material (1) and are placed on ferrite E core (4).

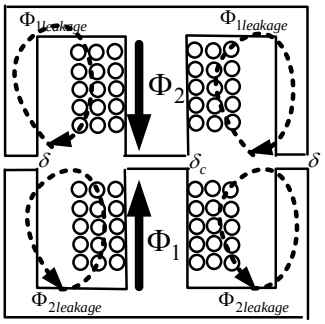

Fig. 3. Core structure of the coupled inductor

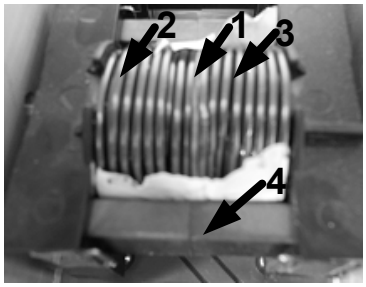

Fig. 4. Practical implementation of the coupled inductor

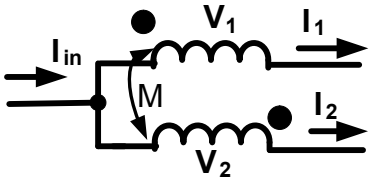

Fig. 5. Circuit of inversely coupled inductors

The basic schematic of a two-phase coupled inductor is shown in Fig. 5. The mutual inductance M represents the coupling between the two inductors. The voltages across the two inductors (V_1, V_2) are related to the currents through them (i_1, i_2) as follows:

(1) $$V_1 = L_1 \frac{di_1}{dt} - M\frac{di_2}{dt}$$

(2) $$V_2 = -M\frac{di_1}{dt} + L_2\frac{di_2}{dt}$$

Assuming that both inductors have the same inductance $L_1=L_2=L$ and by rearranging the equations (1) and (2):

(3) $$\frac{di_2}{dt} = \frac{V_2}{L} + \frac{M}{L}\frac{di_1}{dt}$$

(4) $$\frac{di_1}{dt} = \frac{V_1}{L} + \frac{M}{L}\frac{di_2}{dt}$$

Substituting (3) in (1) and (4) in (2) is given as:

(5) $$V_1 + \frac{M}{L}V_2 = (L - \frac{M^2}{L})\frac{di_1}{dt}$$

(6) $$V_2 + \frac{M}{L}V_1 = (L - \frac{M^2}{L})\frac{di_2}{dt}$$

Fig 6. shows gating signals of transistors VT1 and VT3. One switching cycle can be divided in four different modes. The transistor VT1 is on in the period a. During this period switch VT3 is in off position and voltages can be expressed as follows:

(7) $$V_1 = V_{IN}\,; V_2 = V_{IN} - V_0$$

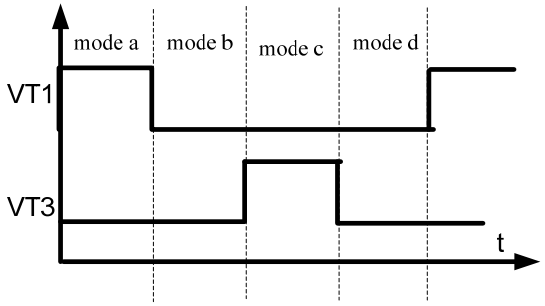

Fig. 6. Signals in one switching cycle

In this stage two phase converter act as single phase boost converter and the output voltage is given as:

(8) $$V_0 = \frac{V_{IN}}{(1-D)}$$

Substituting (8) in (7):

(9) $$V_2 = -\frac{D}{(1-D)}V_1$$

Substituting (9) in (5) and solving for V_1 it gives

(10) $$V_1 = \left(\frac{L - \frac{M^2}{L}}{1 - \frac{M}{L}\frac{D}{1-D}}\right)\frac{di_1}{dt}$$

The equivalent inductance during the period a is

(11) $$L_{eq1,a} = \frac{L - \frac{M^2}{L}}{1 - \frac{M}{L}\cdot\frac{D}{1-D}} = \frac{1-k^2}{1-(k\cdot\frac{D}{(1-D)})}L$$

where k is coefficient of coupling k=M/L.
During time interval b VT1 and VT3 are switched off and V1 and V2 is given as

(12) $$V_1 = V_2 = V_{IN} - V_{out}$$

Substituting (12) in (5) , the equivalent inductance is:

(13) $$L_{eq1,b} = \frac{L - \frac{M^2}{L}}{1 + \frac{M}{L}} = (\frac{1-k^2}{1+k})L = (1-k)L$$

Similarly as in period a during interval c voltages is given as

(14) $$V_1 = V_{in} - V_{out}\,;\; V_2 = V_{in}$$

Substituting (9) in (15), voltage V_2 is

(15) $$V_2 = \frac{1-D}{-D}V_1$$

Substituting (16) in (6) , the equivalent inductance is:

(16) $$L_{eq1,c} = \frac{L - \frac{M^2}{L}}{(1+\frac{M}{L})\frac{1-D}{D}} = \frac{1-k^2}{1-(k\cdot\frac{1-D}{D})}L$$

The interval d is the same as interval b and the equivalent inductance of this period is

(17) $$L_{eq1d} = L_{eq1,b}$$

Second branch is equal to the first one only shifted in phase by 180 degrees, so the corresponding inductances must be equal:

(18) $$L_{eq2a} = L_{eq1,c}$$

(19) $$L_{eq2b} = L_{eq2,d} = L_{eq1,b}$$

(20) $$L_{eq2,c} = L_{eq1,a}$$

The phase current ripples of phase 1 and phase 2 can be expressed with equations from the boost converter basics as

(21) $$\Delta I_{1,a} = \frac{V_{in}D}{f_{sw}L_{eq1,a}} = \frac{V_{in}D}{f_{sw}L}\cdot\frac{1-k\cdot\frac{D}{1-D}}{1-k^2}$$

(22) $$\Delta I_{2,a} = \frac{(V_{in}-V_{out})\cdot D}{f_{sw}L_{eq2,a}} = \frac{V_{in}D\cdot(1-\frac{1}{1-D})}{f_{sw}L_{eq2,a}} = \frac{V_{in}D\cdot(k-\frac{D}{1-D})}{f_{sw}L\cdot(1-k^2)}$$

The overall output current ripple is the sum of two phase current ripples and for inversely coupled inductors it is given as

(23) $$\Delta I_a = \Delta I_{1,a} + \Delta I_{2,a} = \frac{V_{in}D}{f_{sw}L(1-k)}\cdot\frac{1-2D}{1-D}$$

The current ripple for uncoupled inductor case is given as

(24) $$\Delta I_{unc} = \frac{V_{in}D}{f_{sw}L} + \frac{(V_{in}-V_{out})D}{f_{sw}L} = \frac{V_{in}D}{f_{sw}L}\cdot\frac{1-2D}{1-D}$$

The ratio between current ripple of uncoupled inductor and current ripple in case of inversely coupled inductor is

(25) $$\frac{\Delta I_{unc}}{\Delta I_{coupled}} = 1-k$$

Equation 25 shows that output current ripple will be larger in case if inversely coupled inductor is used. But from the other side anyway from Fig. 1 output current ripples will be less than in case of single phase converter if value of duty cycle (D) is near to 0.5.

Pulsations of current in each phase is determined by equivalent inductance $L_{eq1,a}$ if duty cycle is less than 0.5 and $L_{eq1,c}$ if duty cycle is more than 0.5. As can seen from equations (11) and (16), using derivative functions to obtain values of equivalent inductance that minimize current ripple:

(26) $$\frac{L_{eq}}{L} = \frac{1-k^2}{1+C\cdot k}$$

(27) $$\frac{d(\frac{L_{eq}}{L})}{dk} = \frac{-C(k^2+\frac{2}{C}k+1)}{1-Ck^2} = 0$$

where $C = -\frac{1-D}{D}$ if D>0.5 and $C = -\frac{D}{1-D}$ if D<0.5.

Solution of the expression $k^2 + \frac{2}{C}k + 1 = 0$ is given as

(28) $$k_{1,2} = \frac{-\frac{2}{C} \pm \sqrt{\frac{4}{C^2}-4}}{2} = -\frac{1}{C} \pm \sqrt{\frac{1}{C^2}-1}$$

Table 1. Coupling coefficient to minimize per-phase current ripple

D	C	k
0,1	-0,11	0,06
0,2	-0,25	0,13
0,3	-0,43	0,23
0,4	-0,67	0,38
0,5	-1,00	1,00
0,6	-0,67	0,38
0,7	-0,43	0,23
0,8	-0,25	0,13
0,9	-0,11	0,06

Table 1 shows optimal coupling coefficient (k) according to duty cycle D calculated by equation 28. In this case duty cycle of the DC/DC converter will be from 0.4 to 0,6 so the optimal coupling coefficient from to eliminate current ripple in each phase is near to 0,7.

When a load current change occurs, the period of operation of mode a changes. Let this period change be ΔD. In the coupled inductor case, the relation of current change Δi to load current change can be written as:

(29) $$\Delta i = \frac{V_{in}}{f_{sw}L_{eq,b}}\Delta D$$

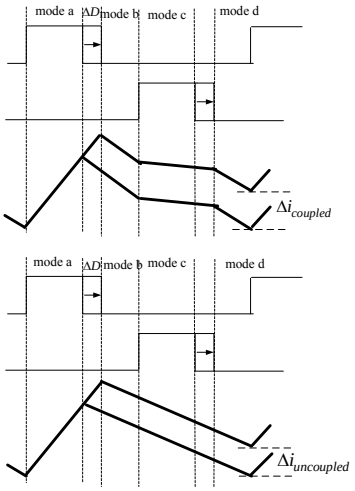

Fig. 7. Current change in transient process [10]

Figure 7 shows comparison of load current transient response of inductor current with and without coupling between inductors. Here we can see that the current change Δi in coupled inductor case is larger than with no inductor coupling. It means that coupled inductor enable faster current change response. From (13) and (29) can be concluded that transient response time is determined only by value L(1-k). So larger coupling coefficient improves speed of transient response.

The DC/DC converter is proposed to power of 2 kW and maximum output voltage is 270 volt and rated output current 5 A. The voltage of wind generator V_{in} is variable and it changes from 30 to 150 V. Inductor is wound on ETD39 coil former, it structure is shown in Fig. 4. The central air gaps is selected equal to δ_C=1,4 mm, but air gap

of outer legs is equal to δ=0,25 count of windings is 80, the measured inductance is L=830 μH, coupling coefficient k=0,7.

Fig. 8. Measuring of inductance

It is difficult to calculate precise value of inductance and coupling coefficient therefore easier is measure this values and change parameters of the inductor (air gaps, winding count) to achieve desired values. To measure coupling coefficient both windings must be connect in series and measured total inductance of this connection (Fig. 8). This inductance can be expressed as follows.

(30) $$L_{total} = L_1 + L_2 + 2M$$

If both of inductances is equal (L_1=L_2=L) then mutual inductance can be expressed as:

(31) $$M = \frac{L_{total} - 2L}{2}$$

Coupling coefficient is equal to:

(32) $$k = \frac{M}{L}$$

Table 2. Per-phase inductance depending on duty cycle

D	Leq/L
0,4	0,96
0,425	1,06
0,45	1,19
0,475	1,39
0,5	1,70
0,525	1,39
0,55	1,19
0,575	1,06
0,6	0,96

Table 2 shows results of the equivalent inductance in case of coupled inductor relationship to inductance without coupling calculated by equation 26. This relationship is proportional to the current ripple reducing in each phase in respect to uncoupled inductor case. If duty cycle is equal to 0.6 the current ripple is the larger than in case of uncoupled inductor but by duty cycle 0,5 current ripple will be 1,7 smaller. The benefits from coupled inductor in this case is small size of inductor, fast transient response and reduced current ripple in inductor for some duty cycles.

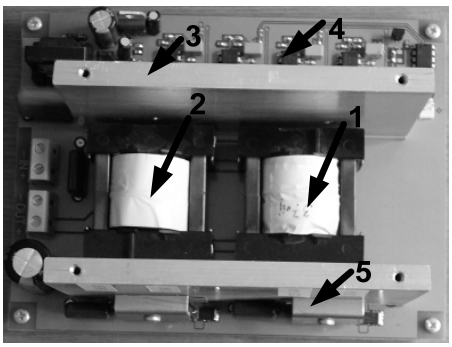

Fig. 9. Hardware implementation of DC/DC converter

Figure 9 shows hardware implementation of digitally controlled boost DC-DC converter with coupled inductor. The power transistors and diodes (5) are placed on the radiator plate (3). The pulse width modulated signals from the microcontroller board goes to the MOSFET drivers (4). The inductors (1 and 2) is designed by using the ETD core.

Conclusions

Digitally controlled boost converter with coupled inductor for wind turbine generator matching with industrial converter is proposed. Inversely coupled structure of inductor allows increasing transient responding time, reducing size of inductor and reducing current ripple of inductor in some modes. Interleaved structure of DC-DC boost converter reduce output current ripple.

The coupled inductor is designed in convenient way by using ETD39 coil former. In paper is proposed method how to measure coupling coefficient and in simple way by changing air gap and winding count get necessary inductance and coupling coefficient.

Acknowledgements. *This research work has been supported by Latvian Council of Science (Project Nr. 673/2014).*

REFERENCES

[1] *Taylor R*. PowerLab Notes: *When to choose multiphase* [online] [16.05.2014.]. Available at http://e2e.ti.com/blogs_/b/powerhouse/archive/2013/10/31/powerlab-notes-when-to-choose-multiphase.aspx?DCMP=powerlab&HQS=pwr-powerlab-pwrhouse-20140116-multiphase-blog-en.

[2] *Ashur A. S., Thorn R.* Modeling and Simulation of Automotive Interleaved Buck Converter. *Universities Power Engineering Conference,* 2009, pp. 1-6.

[3] *Chunliu C., Chenghua W.* Research of an Interleaved Boost Converter with four *Interleaved Boost Convert Cells. Microelectronics* & Electronics, 2009, pp. 396–399.

[4] *Huber L., Irving B. T., Jovanovic M. M.* Open-Loop Control Methods for Interleaved DCM/CCM Boundary Boost PFC Converters. *IEEE Transactions on Power Electronics*, *23*(4), 2008, pp. 1649–1657.

[5] *Pit-Leong W., Peng X., Yang P.* Performance improvements of interleaving VRMs with coupling inductors, *IEEE Trans. Power Electronics,* Vol. 16, No. 4, 2001, pp. 499-507.

[6] *Wong P.* Performance Improvement Of Multi-Channel Interleaving Voltage Regulator Modules With Integrated Coupling Inductors, Ph.D. dissertation, *Dept. Electr.Comput. Eng*., Virginia Tech, Blacksburg, 2001.

[7] *Vinnikov, D.; Roasto, I.; Zakis, J.; Strzelecki, R.* New Step-Up DC/DC Converter for Fuel Cell Powered Distributed Generation Systems: Some Design Guidelines. Przeglad Elektrotechniczny, 86(8), 2010, pp. 245 - 252.

[8] *Zhu G., Wang K.* Modeling and design considerations of coupled inductor converters, *Applied Power Electronics Conference and Exposition (APEC)*, 2010., pp.7-13.

[9] *Lee P., Lee Y., Cheng D.., Liu X.* Steady-state analysis of an interleaved boost converter with coupled inductors, *Industrial Electronics, IEEE Transactions on* , vol.47, no.4, 2000., pp.787-795.

[10] *Santhos A., et al.* Analysis of coupled inductors for low-ripple fast-response buck converter. *IEICE transactions on fundamentals of electronics, communications and computer sciences* vol. 92, no.2, 2009., pp. 451-455.

Authors*: M.sc. Kaspars Kroics, E-mail: kaselt@inbox.lv; M.sc. Ugis Sirmelis, E-mail: ugis.sirmelis@gmail.com; as. prof. Viesturs Brazis, E-mail: viesturs.brazis@rtu.lv; Institute of Physical Energetics, Laboratory of Power Electronics, Aizkraukles 21, LV-1006, Riga, Latvia; Riga Technical University, Institute of Industrial Electronics and Electrical Engineering, Kronvalda 1, LV-1010, Riga, Latvia.*